Catal Lett (2007) 118:180–186
DOI 10.1007/s10562-007-9216-4

Low-temperature Oxidation of Carbon Monoxide on Co/ZrO_2

Matthew M. Yung · Erik M. Holmgreen · Umit S. Ozkan

Received: 4 June 2007 / Accepted: 11 July 2007 / Published online: 25 July 2007

Abstract A 10%Co/ZrO_2 catalyst prepared by impregnation was tested for its activity for the oxidation of CO to CO_2 in excess oxygen. Activity tests showed that conversion could be obtained at temperatures as low as 20 °C. Time-on-stream studies showed no loss of activity in these experiments, indicating that this catalyst is stable in the experimental oxidizing conditions. The activation energy for the CO to CO_2 oxidation reaction was calculated as E_a = 54 kJ/mol over this catalyst. Characterization of the material by thermogravimetric analysis, temperature-programmed techniques, X-ray photoelectron spectroscopy, and laser Raman spectroscopy indicate that Co_3O_4 is present on monoclinic ZrO_2 after the calcination of the catalyst.

Keywords CO oxidation · Cobalt · ZrO_2 · Co/ZrO_2 · Co_3O_4

1 Introduction

Carbon monoxide is a pollutant that is emitted from many sources. There are numerous applications for which a catalyst capable of oxidizing carbon monoxide to carbon dioxide at low temperatures is desirable. Carbon monoxide can form as a result of incomplete combustion of carbon-containing materials. For automotive applications, the majority of all emissions (80–90%) are released during the "cold-start" period [1] and materials that have high activity at lower temperatures could help to alleviate pollution from this route. The production of high purity hydrogen streams through preferential oxidation of CO (PROX) is another area that has recently garnered much attention for low temperature CO oxidation catalysts [2]. Other applications for low temperature CO oxidation catalysts could consist of indoor air purification, the removal of CO from closed-cycle CO_2 lasers [3], and low temperature hydrocarbon combustion.

Some precious metals such as Pt, Pd and Au [4–6] are well known oxidation catalysts and have received significant attention in emission control catalysis. One significant drawback to these materials, however, is their high cost. To address this concern, a search for lower cost, alternative materials has led to the study of transition metal catalysts. Mechanistic studies on CO oxidation in excess O_2 were carried out and showed cobalt to be an active metal for the reaction, though carbonate formation could lead to decreased activity at temperatures below 100 °C [7]. Other studies have shown strong promotional effects of Co and Fe to Pt/Al_2O_3 catalysts, leading to substantial activity gains for the PROX reaction [8–11]. Studies without Pt, using solely Co, indicate that Co_3O_4 is active for CO oxidation but that the bulk cobalt oxide may reduce to metallic Co^0 under the excess H_2 atmosphere [12, 13]. These studies indicate that a highly oxidized form of cobalt that exhibits strong interaction with a defect-forming support that allows CO activation, such as ZrO_2 or CeO_2, could lead to high activity for the preferential oxidation of CO in excess O_2.

Jansson et al. have also studied cobalt catalysts, Co_3O_4/Al_2O_3 and Co_3O_4, for the low temperature oxidation of CO and reported high initial activity, but observed a deactivation by CO for which they proposed mechanisms involving a partial reduction of cobalt sites, deposition of carbonates, and surface reconstruction [1, 14]. They found,

M. M. Yung · E. M. Holmgreen · U. S. Ozkan (✉)
Department of Chemical and Biomolecular Engineering, The Ohio State University, Columbus, OH 43210, USA
e-mail: ozkan.1@osu.edu

though, that the rate of deactivation could be mitigated or eliminated by operating at elevated temperatures or by increasing the ratio of O_2/CO.

In this paper, we report on the CO oxidation activity for a Co/ZrO_2 catalyst in excess oxygen. In a previous study, we have shown Co/ZrO_2 to possess high activity for oxidation of NO and hydrocarbons in excess oxygen [15, 16]. This catalyst is a good candidate because Co_3O_4 has been shown to be active for CO oxidation and is less expensive than Au and Pt. Zirconia provides enough interaction with the active phase to prevent aggregation and formation of large particles that lead to surface area loss, but the interaction is not so strong that it favors bond formation with the active phase, which would prevent the formation of the active compound [17].

2 Experimental

2.1 Catalysts Synthesis

The catalyst used in these investigations was prepared using incipient-wetness impregnation of ZrO_2 provided by Saint Gobain (Lot #2000920047). The pelletized ZrO_2 support was ground to a powder, sieved in order to obtain particles ranging from 100 to 150 mesh (250–170 μm), and calcined in air at 500 °C for 3 h. Cobalt (10 wt%) was added to the powdered support by dissolving the nitrate precursor, $Co(NO_3)_2 \cdot 6H_2O$ (Aldrich), in an aqueous solution and performing the impregnation using a solution volume equivalent to the total support pore volume. The impregnation was performed in three steps, with the catalyst being dried in air at 110 °C between impregnations. Following the final drying, the catalyst was heated at a ramp rate of 10 °C/min to 500 °C and calcined in air for 3 h.

2.2 Catalyst Activity Testing

Steady-state reaction experiments were performed in a stainless steel, fixed bed flow reactor (1/4″ O.D.) at atmospheric pressure. The catalyst (200 mg unless otherwise specified) was held in place between two quartz wool plugs. Various concentrations of feed gases provided by Praxair (CO, O_2, He) were sent to the reactor to obtain a feed flow rate of Q_{tot} = 45 cm^3 (STP)/min, corresponding to a typical space velocity of 35,000 h^{-1}. Flow rates were controlled using Brooks 5850E mass flow controllers. Before the reaction, the samples were pretreated in 10% O_2 at 300 °C for 30 min. Temperatures were measured using Omega K-type thermocouples, and adjusted using a PID temperature controller (Omega CN 49000). Analysis of the feed and effluent gas streams was performed using a gas chromatograph (Varian Micro-GC, Model CP 4900) equipped with molecular sieve 5A and Porapaq Q columns.

2.3 Catalyst Characterization

N_2 physisorption experiments at 77 K were performed on a Micrometrics ASAP 2010 accelerated surface area and porosimetry system. The sample was degassed at 130 °C for at least 8 h and the BET surface area and pore volume was determined for the catalyst. The unloaded ZrO_2 powder had a pore volume of 0.25 mL/g and surface area of 48 m^2/g, which decreased after cobalt addition to 41 m^2/g for the 10%Co/ZrO_2 catalyst. In order to quantify the number of adsorption sites on the oxide catalyst, methanol adsorption was conducted [18–20]. A six-port valve using a sample 1 mL sample loop was used to pulse methanol to the sample 50 °C, using an on-line quadrupole mass spectrometer (Cirrus RGA) for monitoring. The methanol uptake on 10%Co/ZrO_2 was determined to be 3.65 μmol/m^2.

X-ray photoelectron spectroscopy (XPS) was performed using an AXIS Ultra equipped with a monochromatic aluminum X-ray source. The sample was degassed in the transfer chamber overnight to reach a pressure of 10^{-6} torr, and it was then moved to the analysis chamber, for operation at 10^{-9} torr. A survey scan covering the entire binding energy range was performed to confirm the expected peaks before more detailed scans for the elements of interest were performed. The standard location of the carbon 1s binding energy peak, 284.5 eV, was used for charge shift corrections, and peak deconvolution was performed using the GRAMS software package.

Thermogravimetric analysis (TGA) was performed to examine the weight changes associated with precursor decomposition and crystalline structure formation during calcination of the freshly synthesized catalyst. Approximately 90 mg of catalyst was loaded into the platinum sample crucible and heated in an air flow of 15 cm^3/min at a rate of 5 °C/min from 15 to 700 °C and held for 30 min. A Setaram TG-DSC111 was used to obtain simultaneous TGA and differential scanning calorimetry (DSC) information during the catalyst calcination. During this experiment, an MKS Instruments Cirrus quadrupole mass spectrometer with a heated capillary inlet line was used to monitor the effluent gas downstream of the catalyst sample. X-ray diffraction (XRD) patterns were acquired on the sample for phase identification during calcination using a Bruker D8 Advance X-ray diffractometer equipped with a Cu K_α source with wavelength 1.54 Å. The presence of a stable monoclinic ZrO_2 phase and Co_3O_4 were observed [16.]. Laser Raman spectroscopy was performed in ambient conditions on powdered samples with a Horiba Jobin-Yvon LabRam HR800 spectrometer in the backscattering geometry. The

excitation source was a 514.5 nm argon ion laser (Coherent Innova I70C-5) and the power, measured at the sample, was set to 2.0 mW.

Temperature programmed reaction experiments were conducted to examine catalyst behavior over the temperature window of interest. Catalyst samples of 100 mg were loaded between two quartz wool plugs in a quartz U-tube reactor. The reactor is placed in an electrically heated furnace controlled by an Omega CSC32 temperature controller and an Omega K-type thermocouple. Gas flow rates were controlled by Brooks 5850E mass flow controllers and total gas flow rates were 30 mL/min. The feed gas consisted of 5,000 ppm CO, 1% O_2, and 2% H_2O (when present) in balance He. The feed was introduced to the sample and allowed to equilibrate before the temperature ramp at 2 °C/min was performed from 20 to 300 °C. To prevent condensation of any H_2O, the stainless steel lines upstream and downstream of the reactor were heated using heating cords controlled by a Variac voltage controller. The analysis of gas phase products and reactants was conducted by monitoring the effluent with a Thermo-Finnigan DSQ GC/MS mass spectrometer. In order to attribute various mass-to-charge (m/z) signals to a particular molecular species, corrections were made to eliminate interference caused from molecular fragmentation due to the electron impact ionization process.

3 Results

3.1 TGA-DSC-MS

The calcination process of the freshly prepared catalyst was examined using TGA-DSC-MS. The mass change and heat flow were monitored with TGA/DSC while the gas species in the effluent stream were simultaneously tracked using mass spectrometry during a temperature-programmed calcination of the catalyst. The m/z ratios of 12, 16, 17, 18, 28, 30, 32, 44, and 46 were monitored, though some signals showed no significant deviation from their baseline values and are not displayed. Figure 1(a) shows the mass changes and heat flow during calcination of the 10%Co/ZrO_2 catalyst. The mass change from 89.7 to 86.2 mg represents a 3.9% loss in mass. Nitrate decomposition from the cobalt nitrate precursor should comprise 3.2% of the dried, pre-calcined catalyst mass and the additional mass losses can be primarily attributed to water desorption. The two sharp endothermic peaks in the DSC signal around 100 °C and 300 °C correspond to the desorption and decomposition of water and nitrates, respectively, which is evident from the simultaneous mass spectrometry data for the m/z signals of 17, 18, and 30 shown in Fig. 1(b). The water

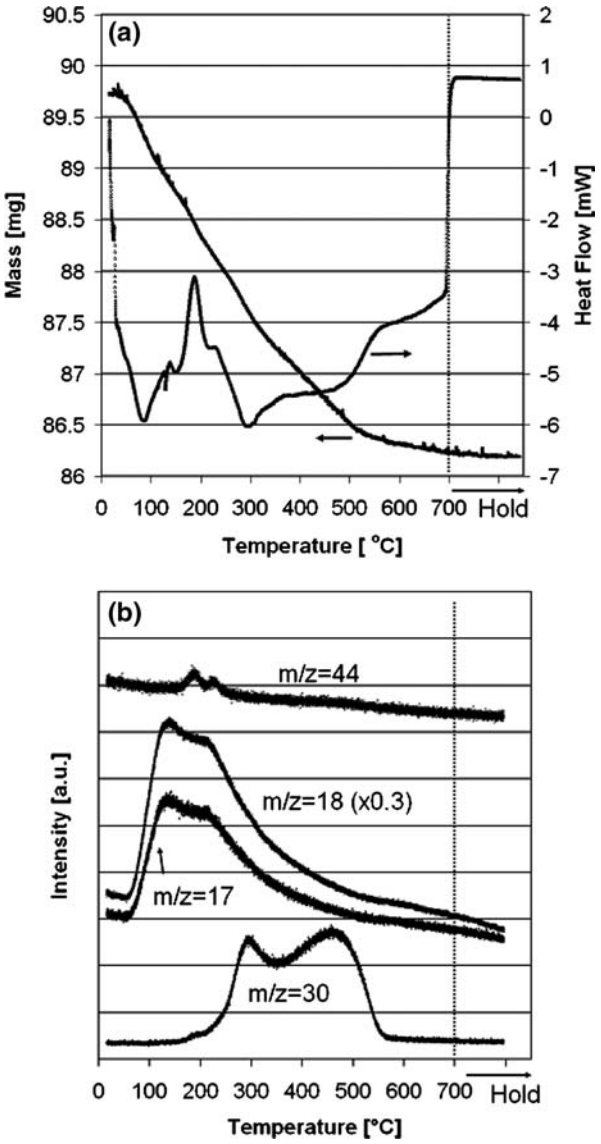

Fig. 1 In-air calcination of dried 10%Co/ZrO_2 with monitoring of the (**a**) TGA/DSC signals and (**b**) mass spectrometry effluent

desorption takes off rapidly once the temperature ramp is initiated and starts to decrease above 200 °C. Two small peaks in the m/z = 44 signal are attributed to the loss of CO_2 adsorbed from the atmosphere. The nitrates from the cobalt precursor, indicated by m/z = 30 in Fig. 1(b), exhibit a decomposition feature centered at 475 °C during the temperature-programmed calcination. This indicates that the 3 h hold period at 500 °C during the synthesis of this catalyst will decompose the cobalt nitrate precursor. No high temperature (>500 °C) event was observed in the mass or heat flow signals, which could arise from interaction between the cobalt and ZrO_2, indicating that no cobalt–zirconium phase is formed, which is consist with XRD results [16].

3.2 Activity Measurements

Time-on-stream studies at room temperature (20 °C) were conducted on the 10%Co/ZrO_2 catalyst using feed streams containing 600 ppm and 1,900 ppm CO and 10% O_2, respectively, in balance He. Figure 2 shows the concentrations of CO and CO_2 during the experiment using a feed stream of 45 sccm. Complete conversion of CO to CO_2 was obtained and no decline in conversion was observed over the course of this experiment. Complete conversion of CO to CO_2 was also observed when during the experiment in which the feed concentration of CO was 600 ppm (data not shown).

To further study the catalyst's activity, an additional experiment was conducted using a substantially higher concentration of CO (1.5%) with 10% O_2 in balance He. The carbon and oxygen balances were >99% and CO_2 was the only product that was formed. During this experiment, the temperature was increased by temperature increments of 5–10 °C. The concentrations of CO and CO_2 during this experiment are shown in Fig. 3. The higher CO concentration in the experiment required elevated temperatures in order to achieve complete conversion of CO, which was obtained at 135 °C. The experiment was run over the course of several days and the catalyst was shown to be stable during the course of the experiment, with no decline in activity at any of the reported temperatures. Using methanol adsorption for site quantification, the turn over frequency (TOF) data were used to prepare the Arrhenius plot shown in Fig. 4, and the activation energy for oxidation of CO to CO_2 over 10%Co/ZrO_2 was calculated as 54 kJ/mol.

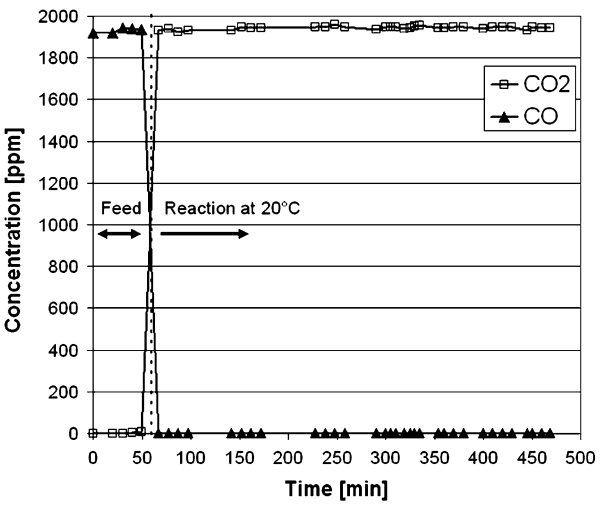

Fig. 2 Time-on-stream study of CO oxidation over 10%Co/ZrO_2. Reaction conditions: 1,900 ppm CO, 10% O_2, balance He, Q_{tot} = 45 sccm, 200 mg catalyst

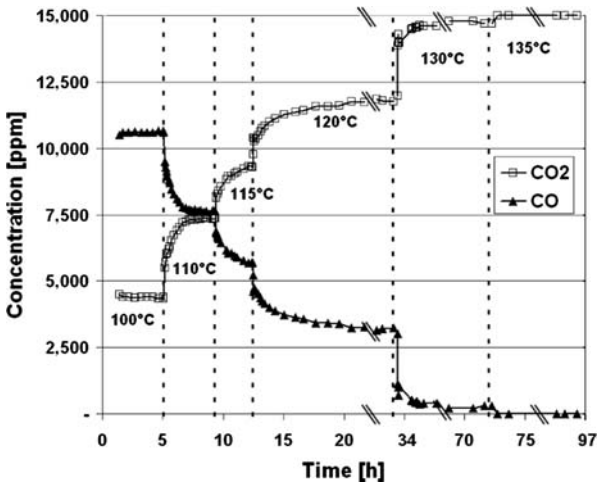

Fig. 3 Effects of time and temperature on CO oxidation over 10%Co/ZrO_2. Reaction conditions: 1.5% CO, 10% O_2, balance He, Q_{tot} = 45 sccm, 200 mg catalyst

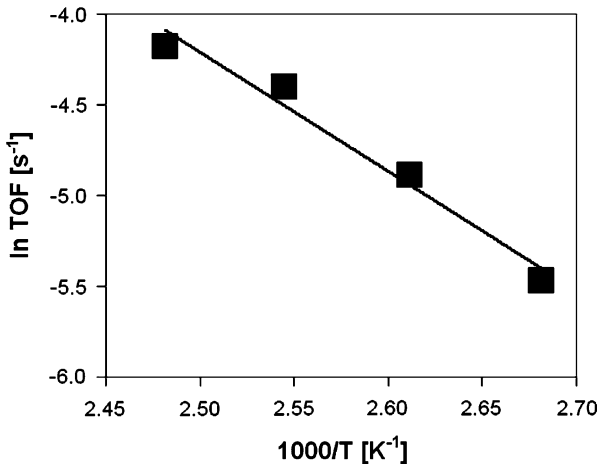

Fig. 4 Arrhenius plot for CO oxidation over a 10%Co/ZrO_2 catalyst

In order to examine the effect of water on the oxidation of CO over this catalyst, temperature-programmed reaction studies were performed with and without the presence of water vapor, using mass spectrometry for product monitoring. The corrected ion mass-to-charge signals corresponding to the CO and CO_2 during these experiments are displayed in Fig. 5. It can be observed that the decrease in CO concentration is accompanied by the simultaneous increase in CO_2 concentration. Figure 5(a) shows that complete conversion of CO is achieved around 135 °C. When water was present, however, there appeared to be some inhibition effect, with temperature required for complete CO conversion shifting by about 50 °C. Figure 5(b) shows that complete conversion of CO was not obtained until about 185 °C, possibly due to a competitive adsorption effect.

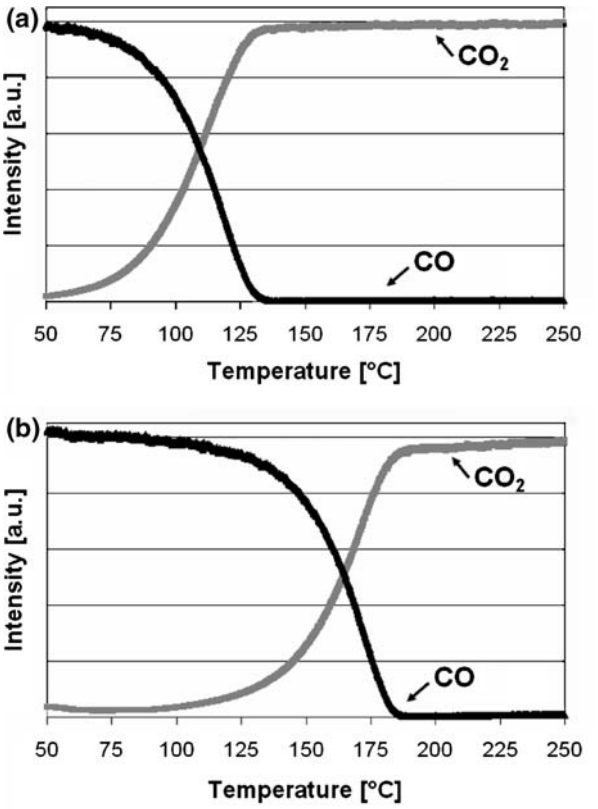

Fig. 5 Temperature-programmed reaction on 10%Co/ZrO_2 using 100 mg catalyst, Q_{total} = 30 sccm, 5,000 ppm CO, 1% O_2, balance He in (**a**) 0% H_2O and (**b**) 2% H_2O

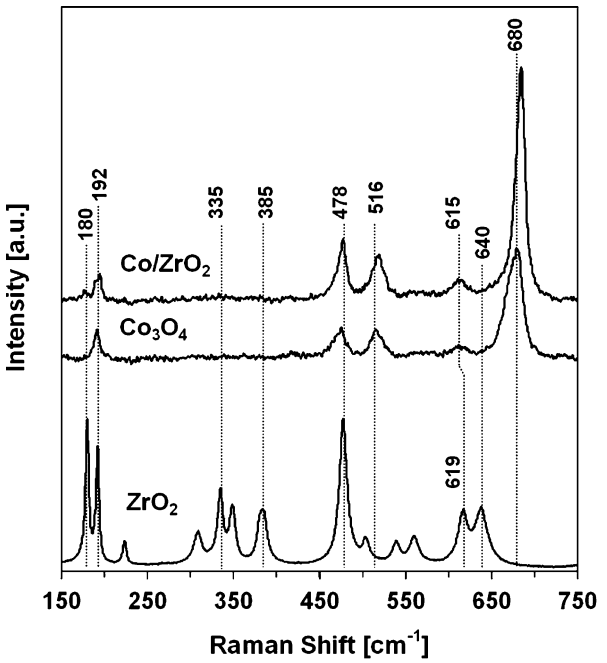

Fig. 6 Laser Raman spectroscopy on Co/ZrO_2, Co_3O_4, and ZrO_2 using a 514.5 nm excitation source

3.3 Laser Raman Spectroscopy

Structural information on the catalyst was obtained using laser Raman spectroscopy. Figure 6 shows the spectra obtained on the powdered 10%Co/ZrO_2 catalyst, ZrO_2 support, and bulk Co_3O_4. Strong bands typical of monoclinic ZrO_2 were observed on the ZrO_2 support at Raman shifts of 180, 192, 335, 385, 478, 619, and 640 cm^{-1} [21–23]. Bands at 192, 475, 516, 615, and 680 cm^{-1} are consistent with those previously reported for Co_3O_4 [21, 24, 25]. The laser Raman spectra on the Co/ZrO_2 catalyst looks quite similar to that of the reference Co_3O_4, although contributions from ZrO_2 are evident at 180 and 478 cm^{-1}. These results indicate that cobalt is present as Co_3O_4 in the Co/ZrO_2 catalyst. The lack of clearly visible vibrational bands from the ZrO_2 support in the Co/ZrO_2 sample can be explained by the smaller Raman cross-section of monoclinic ZrO_2 as compared to Co_3O_4 [26].

3.4 X-ray Photoelectron Spectroscopy

The XPS spectra of various regions from the 10%Co/ZrO_2 catalyst are shown in Fig. 7. Figure 7(a) shows the Zr 3d region, and the two characteristic Zr $3d_{3/2}$ and $3d_{5/2}$ peaks at 184.0 and 181.6 eV, respectively, arise from monoclinic ZrO_2 [27–29]. The O 1s signal, along with the deconvoluted peaks and their summation, are shown in Fig. 7(b). The O 1s peak at 529.7 eV is characteristic of metal oxides and can be attributed to O^{2-} on the ZrO_2 surface, while the peak at 531.4 eV has commonly been attributed to O^- and OH^- [30]. Figure 7(c) shows the Co 2p region for the catalyst. The Co $2p_{3/2}$ and Co $2p_{1/2}$ peaks are consistent with both Co^{3+} and Co^{2+} since the binding energy difference between Co^{3+} and Co^{2+} is only 0.9 eV, with Co^{2+} at the higher binding energy [31, 32]. Shake up peaks located at 6 eV higher binding energies than the main Co 2p peaks can be used to identify the presence of Co^{2+}. No clear shake up peaks were observed, indicating that cobalt is mostly present as Co^{3+}, which would be consistent with the presence of Co_3O_4 in which 2/3 of Co is in 3+ oxidation state. XPS spectra of bulk Co_3O_4 with no clear shake-up peaks have been reported previously [33–35].

4 Conclusions

The present work demonstrates that an active Co/ZrO_2 catalyst for CO oxidation can be synthesized using the incipient wetness impregnation technique. Activity measurements showed that substantial conversion of CO to CO_2 could occur, even at room temperature. Time-on-stream studies in excess oxygen showed no decline in activity during the

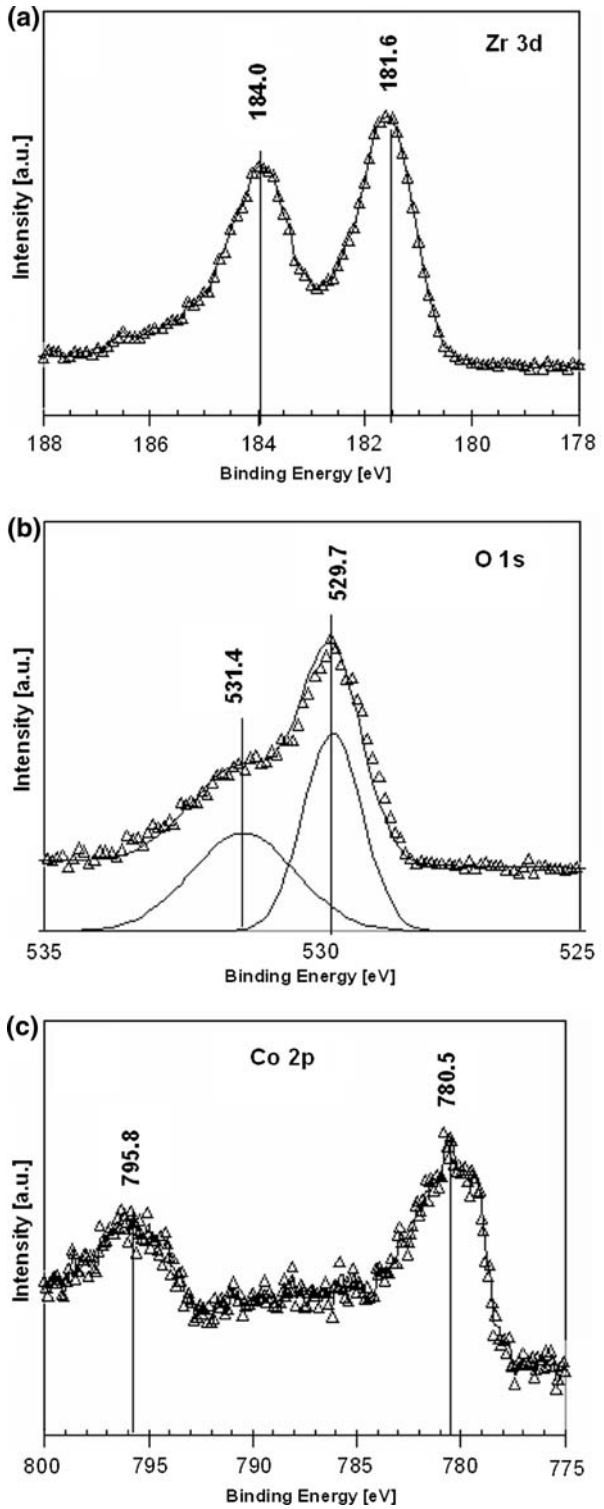

Fig. 7 XPS spectra on 10%Co/ZrO_2, (**a**) Zr 3d region, (**b**) O 1s region, and (**c**) Co 2p region

course of the experiments. Characterization studies for phase identification indicate that cobalt is present as Co_3O_4 on a monoclinic ZrO_2. Temperature programmed reaction studies showed that the presence of 2% water vapor led to some inhibition of the CO oxidation reaction. In addition to the current work, this catalyst is being evaluated for the preferential oxidation of CO in the presence of hydrogen and has shown promising initial results.

Acknowledgements The financial support provided for this work by the Ohio Coal Development Office and the Ohio Department of Development through a Wright Center of Innovation is gratefully acknowledged. The authors would also like to acknowledge NSF support for acquisition of the XPS system under NSF-DMR grant #0114098.

References

1. Jansson J, Palmqvist AEC, Fridell E, Skoglundh M, Osterlund L, Thormahlen P, Langer V (2002) J Catal 211:387
2. Ghenciu A (2002) Curr Opin Solid State Mater Sci 6:389
3. Mirkelamoglu B, Karakas G (2006) Appl Catal A Gen 299:84
4. Liu W, Flytzani-Stephanopoulos M (1995) J Catal 153:304
5. Choudhary TV, Goodman DW (2002) Top Catal 21(1–3):25
6. Yan Z, Chinta S, Mohamed AA, Fackler JP Jr, Goodman DW (2006) Cat Lett 111 (1–2):15
7. Wang C, Tang C, Tsai H, Kuo M, Chien S (2006) Catal Lett 107:31
8. Gracia F, Li W, Wolf E (2003) Catal Lett 91:235
9. Chang B, Lu Y, Tatarchuk B (2006) Chem Eng J 115:195
10. Roberts G, Chin P, Sun X, Spivey J (2003) Appl Catal B Env 46:601
11. Watanabe M, Uchida H, Ohkubo K, Igarashi H (2003) Appl Catal B Env 46:595
12. Omata K, Kobayashi Y, Yamada M (2005) Catal Comm 6:563
13. Ozkara S, Akin A, Misirli Z, Aksoylu A (2005) Turkish J Chem 29:219
14. Jansson J (2000) J Catal 194:55
15. Holmgreen EM, Yung MM, Ozkan US (2007) Appl Catal B Environ 74:73
16. Yung MM, Holmgreen EM, Ozkan US (2007) J Catal 247:356
17. Colonna S, De Rossi S, Faticanti M, Pettiti I, Porta P (2002) J Mol Catl A: Chem 180:161
18. Badlani M, Wachs IE (2001) Catal Lett 75:137
19. Burcham LJ, Briand LE, Wachs IE (2001) Langmuir 17:6164
20. Briand LE, Farneth WE, Wachs IE (2000) Catal Today 62:219
21. Xiao T, Ji SJ, Wang H, Coleman KS, Green MLH (2001) J Mol Catal A 175:111
22. Li C, Li M (2002) J Raman Spectrosc 33:301
23. Holmgreen EM, Yung MM, Ozkan US (2007) J Mol Catal A Chem doi: 10.1016/j.molcata.2007.01.030, in press
24. Brik Y, Kacimi M, Ziyad M, Bozon-Verduraz F (2001) J Catal 202:118
25. Brik Y, Kacimi M, Bozon-Verduraz F, Ziyad M (2002) J Catal 211:470
26. Gajovic A, Djerdj I, Furic K, Schlogl R, Su DS (2006) Cryst Res Technol 41:1076
27. Quaschning V, Deutsch J, Druska P, Niclas H-J, Kemnitz E (1998) J Catal 177:164
28. Zeng HC, Lin J, Teo WK, Loh FC, Tan KL (1995) J Non-Cryst Solids 181:49
29. Tsunekawa S, Asami K, Ito S, Yashima M, Sugimoto T (2005) Appl Surf Sci 252:1651
30. Zeng HC, Lin J, Teo WK, Wu JC, Tan KL (1995) J Mater Res 10(3):545
31. Pietrogiacomi D, Tuti S, Campa MC, Indovina V (2000) Appl Catal B 28:43

32. Epling WS, Hoflund GB, Weaver JF (1996) J Phys Chem 100:9929
33. Noronha FB, Perez CA, Schmal M, Frety R (1999) Phys Chem Chem Phys 1:2861
34. Haneda M, Kintaichi Y, Bion N, Hamada H (2003) Appl Catal B 46:473
35. Liotta LF, Di Carlo G, Pantaleo G, Venezia AM, Deganello G (2006) Appl Catal B 66:217